Thiol stress–dependent aggregation of the glycolytic enzyme triose phosphate isomerase in yeast and human cells

Amy E. Ford[a,b], Catherine Denicourt[c], and Kevin A. Morano[a,*]
[a]Department of Microbiology and Molecular Genetics and [c]Department of Integrative Biology and Pharmacology, University of Texas McGovern Medical School at Houston, Houston, TX 77030; [b]MD Anderson UT Health Graduate School of Biomedical Sciences, Houston, TX 77030

ABSTRACT **The eukaryotic cytosolic proteome is vulnerable to changes in proteostatic and redox balance caused by temperature, pH, oxidants, and xenobiotics. Cysteine-containing proteins are especially at risk, as the thiol side chain is subject to oxidation, adduction, and chelation by thiol-reactive compounds. The thiol-chelating heavy metal cadmium is a highly toxic environmental pollutant demonstrated to induce the heat shock response and recruit protein chaperones to sites of presumed protein aggregation in the budding yeast *Saccharomyces cerevisiae*. However, endogenous targets of cadmium toxicity responsible for these outcomes are largely unknown. Using fluorescent protein fusion to cytosolic proteins with known redox-active cysteines, we identified the yeast glycolytic enzyme triose phosphate isomerase as being aggregation-prone in response to cadmium and to glucose depletion in chronologically aging cultures. Cadmium-induced aggregation was limited to newly synthesized Tpi1 that was recruited to foci containing the disaggregase Hsp104 and the peroxiredoxin chaperone Tsa1. Misfolding of nascent Tpi1 in response to both cadmium and glucose-depletion stress required both cysteines, implying that thiol status in this protein directly influences folding. We also demonstrate that cadmium proteotoxicity is conserved between yeast and human cells, as HEK293 and HCT116 cell lines exhibit recruitment of the protein chaperone Hsp70 to visible foci. Moreover, human TPI, mutations in which cause a glycolytic deficiency syndrome, also forms aggregates in response to cadmium treatment, suggesting that this conserved enzyme is folding-labile and may be a useful endogenous model for investigating thiol-specific proteotoxicity.**

Monitoring Editor
Thomas D. Fox
Cornell University

Received: Oct 5, 2018
Revised: Dec 21, 2018
Accepted: Dec 27, 2018

INTRODUCTION

Protein folding and stability are influenced by multiple factors, including the local microenvironment, which is in turn impacted by extracellular conditions such as temperature, pH, nutrient status, and the presence of proteotoxic xenobiotics. The presence of reactive oxygen species (ROS) produced as a byproduct of aerobic metabolism, exposure to oxidants, such as hydrogen or organic peroxides, and highly toxic molecules, including the metals cadmium (Cd) and arsenite (As), have the potential to damage proteins and disrupt protein homeostasis (proteostasis; Sharma *et al.*, 2008; Jacobson *et al.*, 2012; West *et al.*, 2012; Tamás *et al.*, 2014; Weids *et al.*, 2016). Cadmium has the potential to bind sulfur, nitrogen, and oxygen atoms of proteins; however, the dissociation constant for monodentate thiol groups is an order of magnitude greater than that for imidazole or carboxyl moieties, suggesting that exposed protein cysteines are likely a primary target for cadmium toxicity. In support of this prediction, yeast mutants defective in protein quality control, including those deficient in ubiquitin-conjugating enzymes or proteasome activity, are hypersensitive to cadmium (Jungmann *et al.*, 1993). Consistent with these findings, cadmium treatment was recently demonstrated to induce protein misfolding and aggregate

This article was published online ahead of print in MBoC in Press (http://www.molbiolcell.org/cgi/doi/10.1091/mbc.E18-10-0616) on January 2, 2019.

*Address correspondence to: Kevin A. Morano (kevin.a.morano@uth.tmc.edu).

Abbreviations used: As, arsenic; PB, P-bodies; QB, Q-bodies; SG, stress granules; UPR, unfolded protein response.

formation as determined by surveillance of the protein chaperone and disaggregase Hsp104 in *Saccharomyces cerevisiae* (Jacobson *et al.*, 2017). As also demonstrated in this study, unlike other proteotoxic stresses such as severe heat shock, cadmium appears to interfere selectively with the folding of nascent polypeptides. The nature of cadmium-induced aggregates and the endogenous yeast proteins sensitive to cadmium and capable of recruiting protein quality control machinery are unknown.

Cells employ dedicated systems to maintain redox balance in different compartments. Redox systems based on the glutathione or thioredoxin pathways shuttle reducing equivalents such as NADPH and glutathione to reduce or form protein disulfides as appropriate (Toledano *et al.*, 2013). Proteins rich in cysteine residues or containing highly reactive cysteines (those prone to formation of a thiolate anion at cellular pH) are especially vulnerable to disruptions in redox balance caused by ROS or nutritional status. Proteomic studies have been undertaken using sophisticated thiol-trapping strategies to identify proteins subject to oxidation in the reductive cytosol in response to either exogenous ROS such as H_2O_2, or to disruption of redox buffering caused by genetic ablation of the thioredoxin system (Le Moan *et al.*, 2006; Brandes *et al.*, 2011). While these studies cataloged the differential effects these manipulations had on the status of protein cysteine residues, their impact on folding or stability remains uninvestigated. Thiol-reactive compounds are potent inducers of transcriptional stress responses. For example, it is well established that reductive thiol stress induces the ER unfolded protein response (UPR; Walter and Ron, 2011). We and others have also demonstrated that thiol oxidants (H_2O_2), organic electrophiles (diamide, celastrol, cyclopentanone prostaglandins), and thiol-chelating metals, including cadmium, activate the heat shock factor 1 (Hsf1)–mediated heat shock response (Trott *et al.*, 2008; Wang *et al.*, 2012). Many of these responses can be blocked by the simultaneous addition of an exogenous reductant, confirming their mode of action.

To better understand proteotoxicity caused by thiol-reactive stress and by the toxic metal cadmium in particular, we sought to identify endogenous yeast proteins whose folding and/or stability is impacted by cadmium, starting from a pool of proteins shown to be susceptible to cysteine oxidation (Le Moan *et al.*, 2006; Brandes *et al.*, 2011, 2013). We carried out a pilot screen using fluorescence microscopy and isolated the glycolytic enzyme triose phosphate isomerase (Tpi1) as an exquisitely cadmium-sensitive, aggregation-prone protein. We demonstrate that cadmium induces aggregation of nascent Tpi1-GFP, with higher doses resulting in greater frequency of aggregation and an increase in the total number of aggregates per cell. Tpi1-GFP colocalizes with Hsp104 and the oxidative stress protein chaperone and peroxiredoxin Tsa1 in structures distinct from stress granules or RNA P-bodies. Two conserved cysteines in Tpi1 are found to confer sensitivity to both cadmium and redox imbalance caused by glucose starvation in aging cells. Finally, we demonstrate that cadmium treatment of the human cell lines HEK293 and HCT116 causes recruitment of the chaperone Hsp70 to cytoplasmic aggregates and induces aggregation of the human TPI enzyme, suggesting that thiol stress–based proteotoxicity is conserved between yeast and humans.

RESULTS

Identification of thiol stress–sensitive, aggregation-prone proteins

Given the recognized propensity of cadmium to interact with reactive thiol groups, we took advantage of previously published studies that identified *Saccharomyces cerevisiae* proteins with reactive cysteine residues (Le Moan *et al.*, 2006; Brandes *et al.*, 2011, 2013). To focus our study, we limited our selections to highly abundant (Ghaemmaghami *et al.*, 2003) nuclear/cytoplasmic proteins to facilitate surveillance via fluorescence microscopy. In addition to 10 candidates obtained from the commercially available ORF-GFP genomic collection (Howson *et al.*, 2005), we included the peroxiredoxin Tsa1, previously shown to localize to cytoplasmic foci under thiol oxidative stress (e.g., H_2O_2) and a strain bearing GFP alone (Jang *et al.*, 2004; Weids and Grant, 2014). Strains were visualized by live-cell fluorescence microscopy following treatment with 100 µM $CdCl_2$ for 1 h. As expected, Tsa1-GFP formed multiple small foci following cadmium treatment, confirming that this cadmium concentration is a cellular thiol stress (Figure 1A). In contrast, the translation factor Eft1-GFP (Figure 1A) and 8 other candidates (Supplemental Figure S1) exhibited a diffuse distribution or no significant change of localization pattern upon cadmium treatment. However, the glycolytic enzymes triose phosphate isomerases (Tpi1-GFP) exhibited substantial focus formation under the same conditions in the majority of cells observed (Figure 1, A and B). Importantly, GFP alone did not form foci, indicating that the fluorescent protein tag itself does not aggregate in the presence of cadmium and is unlikely to confer aggregation on Tpi1. Interestingly, only a fraction of Tpi1-GFP appeared to aggregate and form foci, while the remainder remained diffuse throughout the cytosol. This is in contrast to Tsa1-GFP, which appeared to transition wholly into discrete foci under stress. Together, these findings suggest that misfolding and aggregation of proteins with reactive cysteines is perhaps a rare consequence of

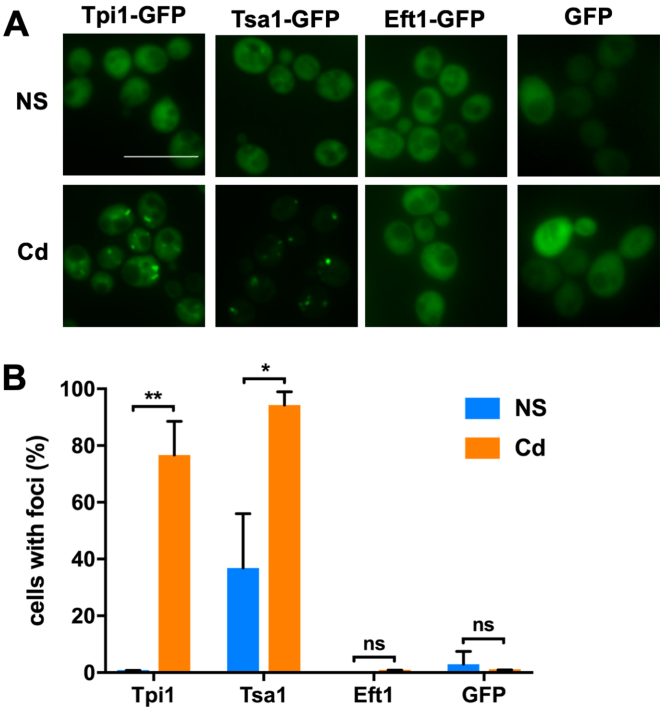

FIGURE 1: The glycolytic enzyme Tpi1 aggregates in response to Cd treatment. (A) Exponentially grown cells bearing genomic GFP–protein fusions of Tpi1, Eft1, and Tsa1 or expressing GFP alone on a plasmid were visualized by live-cell fluorescence microscopy under nonstress conditions (NS) and following treatment with 100 µM Cd for 1 h. Scale: 10 µm. (B) Quantitation of A showing the mean percentages of total cells exhibiting foci ($n = 3$). A minimum of 100 cells were counted per biological replicate. Error bars indicate standard deviation (SD). ns, not significant; *, $p < 0.05$; **, $p < 0.001$.

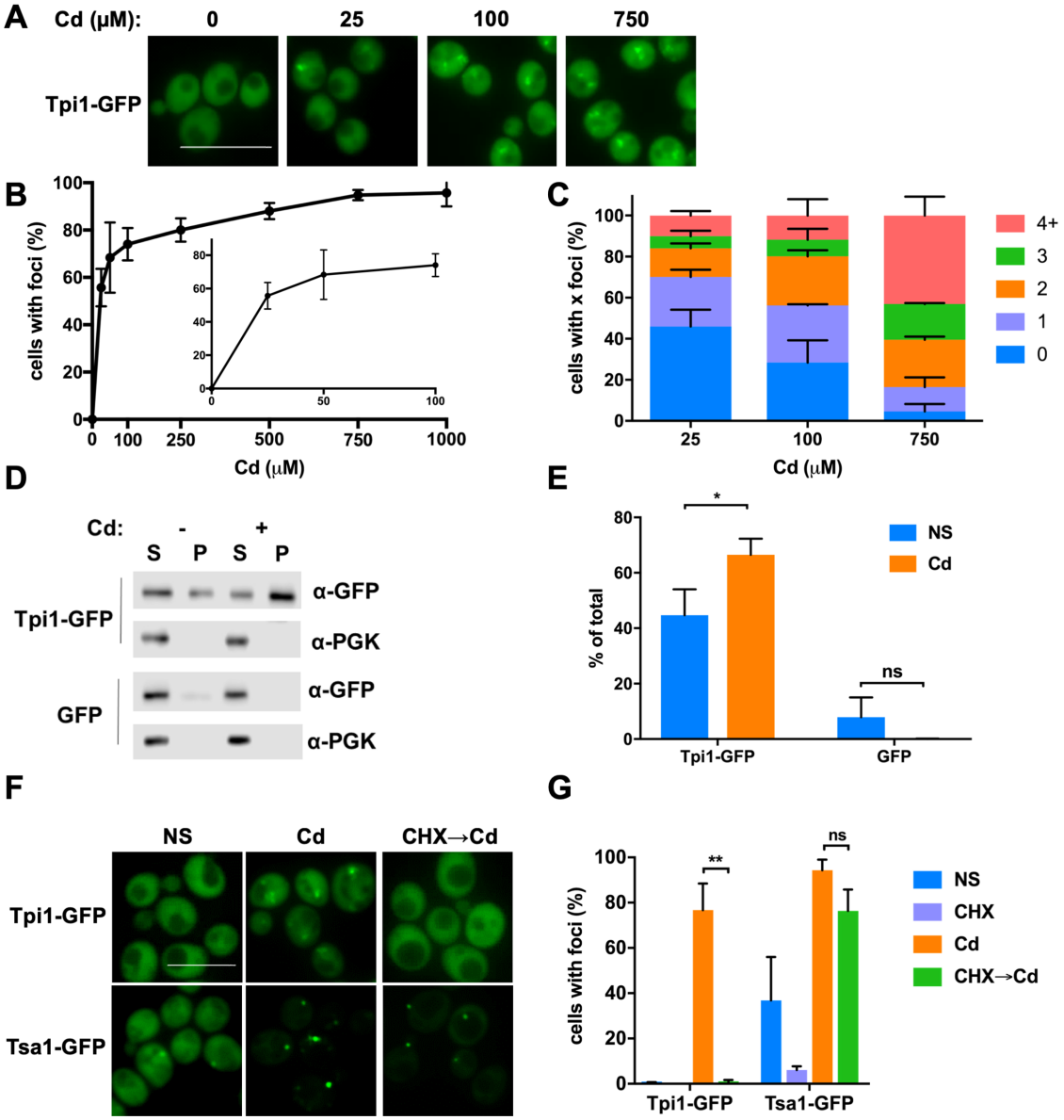

FIGURE 2: Cd-induced Tpi1 aggregation is dose-dependent and only affects newly synthesized protein. (A) Exponentially grown Tpi1-GFP was incubated for 1 h at increasing concentrations of Cd as indicated and visualized by live-cell fluorescence microscopy. Representative images of cells exposed to 0, 25, 100, and 750 μM Cd are shown. Scale: 10 μm. (B) Quantitation of the mean percentage of total cells from A exhibiting foci ($n = 3$). Inset shows gradual increase in number of foci at lower Cd concentrations. (C) Quantitation of the relative percentages of cells from A with 1, 2, 3, or 4+ foci per cell following exposure to 25, 100, and 750 μM Cd. (D) Western blot analysis of soluble (S) and insoluble (P) protein fractions from cells expressing Tpi1-GFP or GFP alone exposed to no (–) or 750 μM (+) Cd for 1 h. S and P fractions were obtained by cryolysis and differential centrifugation as described in *Materials and Methods*. α-GFP monoclonal antibody was used to detect Tpi1-GFP and GFP and a monoclonal α-PGK antibody was used to identify the soluble protein phosphoglycerate kinase as both a fractionation and load control. (E) The mean percentages of P as a fraction of total (S + P) under nonstress (NS, –) and Cd stress conditions from D were quantitated using densitometry ($n = 3$). (F) Exponentially grown cells bearing Tpi1-GFP were visualized by live-cell fluorescence microscopy after no stress (NS), 15 min cycloheximide (CHX), 1 h 100 μM Cd, and 15 min pretreatment with CHX followed by 1 h 100 μM Cd (CHX → Cd). Representative images for NS, Cd, and CHX-Cd only are shown. Scale: 10 μm. (G) Quantitation of the mean percentage of total cells with foci ($n = 3$). A minimum of 100 cells were counted per biological replicate. Error bars indicate SD. ns, not significant; *, $p < 0.05$; **, $p < 0.001$.

thiol stress, despite the previously documented recruitment of Tsa1 and Hsp104 to aggregates in response to cadmium or H_2O_2 treatment (Hanzén *et al.*, 2016; Jacobson *et al.*, 2017). Our findings are consistent with a previous report that only about 20% of cysteine-containing proteins are redox-active (Brandes *et al.*, 2011).

Characterization of Tpi1 thiol stress sensitivity

To further characterize the effects of cadmium-based thiol stress on localization of Tpi1, we incubated the strain bearing Tpi1-GFP for 1 h in increasing concentrations of $CdCl_2$ (0–1000 μM) and visualized aggregate formation by fluorescence microscopy (Figure 2, A–C).

Aggregate formation was observed at 25 μM $CdCl_2$, and both the total fraction of cells with foci and the number of foci per cell increased in a dose-dependent manner. The frequency of focus formation plateaued at 750 μM $CdCl_2$, but even at this concentration, the majority of Tpi1-GFP signal remained diffuse. To confirm that the observed foci represented insoluble protein aggregates, we subjected cells to cryolysis and differential fractionation.

Cells were lysed following a 1-h treatment with 750 μM $CdCl_2$ and supernatant and pellet fractions were obtained, as described in *Materials and Methods*. Protein fractionation was determined by Western blot analysis (Figure 2D). Similarly to what we observed by fluorescence microscopy, GFP alone was found nearly exclusively in the soluble fraction under both nonstress and cadmium treatment conditions. In contrast, we observed approximately 40% fractionation of Tpi1-GFP into an insoluble state in the absence of stress, and a further 20% shift following cadmium treatment as determined by densitometry (Figure 2E). These data suggest that solubility of Tpi1-GFP may be impacted by the fractionation procedure, as few to no aggregates were observed in the absence of stress by fluorescence microscopy. It was previously observed that cadmium-dependent recruitment of Hsp104-GFP to aggregates/foci was blocked by pretreatment of cells with cycloheximide to inhibit protein synthesis, demonstrating that cadmium selectively affects nascent proteins (Jacobson *et al.*, 2017). We therefore treated Tpi1-GFP and Tsa1-GFP cells with 100 μM $CdCl_2$ for 1 h after a 15-min incubation with or without 0.1 mg/ml cycloheximide (Figure 2F). Treatment with cycloheximide alone had no effect on Tpi1-GFP, but completely inhibited Tpi1-GFP aggregation by cadmium. These findings demonstrate that both overall cadmium proteotoxicity, as evidenced by Hsp104 behavior, and folding inhibition of Tpi1 specifically occur solely with nascent polypeptides. This model also explains our observation that a significant fraction of presumably folded and stable Tpi1-GFP remains soluble in the presence of cadmium. Furthermore, cycloheximide pretreatment did not inhibit Tsa1-GFP focus formation, indicating that recruitment of the thiol stress–activated chaperone is unaffected.

We next determined the kinetics of Tpi1-GFP aggregate formation and persistence. Formation of Tpi1-GFP aggregates after the addition of 100 μM $CdCl_2$ was monitored over the course of 3 h at 30-min intervals. Discernable foci were detected within 30 min and nearly all cells observed contained aggregates at 1 h (Figure 3, A–C). Subsequently, the fraction of total cells with aggregates and the number of aggregates per cell diminished and were mostly cleared by 3 h. These data suggest a rapid response to cadmium exposure, followed by slower clearance of the aggregates, suggesting adaptation to the presence of the metal. In addition, we monitored the fate of cadmium-induced Tpi1-GFP aggregates after cadmium washout by visualizing cells exposed to 100 μM $CdCl_2$ for 1 h and then recovered in rich medium lacking cadmium (Figure 3, D and E). In contrast to aggregate dynamics in the presence of cadmium, Tpi1-GFP was completely diffuse throughout the cytosol.

Thiol stress–induced Tpi1 aggregates recruit protein chaperones

Several non-membrane-bound compartments induced after cytotoxic stresses have been identified and their components characterized via fluorescence reporter tagging and microscopy. While proteotoxic stress clearly induces the misfolding of nascent proteins and their subsequent terminal aggregation via hydrophobic interactions, recently a subset of these structures has been found to include mature, folded polypeptides that reversibly localize together as a stress adaptation (Wallace *et al.*, 2015; Saad *et al.*, 2017). Molecular chaperones such as Hsp104 and Tsa1 (in the case of oxidatively damaged proteins) have been utilized to track formation of both types of protein aggregates. These chaperones and other stress-related proteins have been shown to localize into distinct stress foci following different stimuli, including general quality control compartments (Q-bodies, QB), Pub1 to represent formation of stress granules (SG), and Edc3 to indicate processing bodies (PB), the latter two composed of both protein and RNA components (Kshirsagar and Parker, 2004; Buchan *et al.*, 2008). The Q-body is dynamic and has been shown to mature into and integrate with a larger compartment referred to as the JUNQ/INQ (Escusa-Toret *et al.*, 2013; Miller *et al.*, 2015). Because these bodies are closely associated, and the morphology of the cadmium-induced aggregates was inconsistent with the larger JUNQ/INQ compartment, we focused our attention on QB. We likewise excluded an IPOD marker from our analysis, as these structures are morphologically distinct from what we observe with Tpi1 aggregates (Chen *et al.*, 2011). We employed GFP–protein fusions to each of these stress markers and visualized their localization relative to ectopically expressed Tpi1-BFP2 to allow simultaneous two-color surveillance. Under nonstress conditions, Tpi1-BFP2 was diffuse throughout the cytosol, consistent with what we have shown with Tpi1-GFP and indistinguishable from BFP2 expressed alone (Supplemental Figure S2A). We noted that the Tpi1-BFP2 fusion required higher concentrations of $CdCl_2$ to induce aggregation consistently, due possibly to the presence of the wild-type copy of Tpi1 expressed in the genome forming mixed heterodimers. The stress markers Hsp104-GFP, Tsa1-GFP, and Pub1-GFP were likewise primarily diffuse, exhibiting few or no foci (Supplemental Figure S2, B and D). Edc3-GFP formed several foci per cell, consistent with previous studies demonstrating that PB form constitutively under optimal growth conditions (Supplemental Figure S2C). Following a 1-h exposure to 750 μM $CdCl_2$, Tpi1-BFP2 and the stress markers Hsp104-GFP and Tsa1-GFP formed detectable aggregates in response to thiol stress (Figure 4A). Interestingly, Pub1-GFP remained diffuse throughout the cytosol, suggesting that cadmium does not induce the formation of SGs. As evidenced by Edc3-GFP foci, PB were maintained, if not slightly increased, in the presence of cadmium. As we found with GFP, cadmium did not induce aggregation of BFP2 alone (Supplemental Figure S2). To determine the nature of Tpi1 aggregates, we quantified the percentage of colocalization with the indicated stress markers (Figure 4B). Approximately 90% of Tpi1-BFP2 foci colocalized with Hsp104-GFP and Tsa1-GFP foci, demonstrating recruitment of these chaperones. Essentially no colocalization was observed with Edc3-GFP foci, and as stated above, few or no Pub1-GFP foci were induced during cadmium stress. Conversely, only about 30% of Hsp104-GFP and Tsa1-GFP foci were observed to colocalize with Tpi1-BFP2 (Figure 4C). Together, these data strongly support a model where Tpi1 forms QB-type aggregates with the chaperones Hsp104 and Tsa1 that are independent of other known stress-inducible protein structures. Moreover, both Hsp104 and Tsa1 are recruited into additional foci independent of Tpi1, consistent with cadmium causing general proteotoxic stress.

We further examined the temporal association of Tpi1-BFP2 with Tsa1-GFP. Cells treated with 750 μM $CdCl_2$ were harvested from batch culture at 15-min intervals for a total of 1 h and colocalization was determined. We first observed focus formation of Tpi1-BFP2 at 30 min, consistent with what we observed with Tpi1-GFP, while 0–1 Tsa1-GFP foci were present before cadmium treatment (Figure 4, D–F). Between 30 and 60 min, all Tpi1-BFP2 foci colocalized with Tsa1-GFP and increases in both percent of cells with foci and number of foci per cell were coincident. These results are consistent with

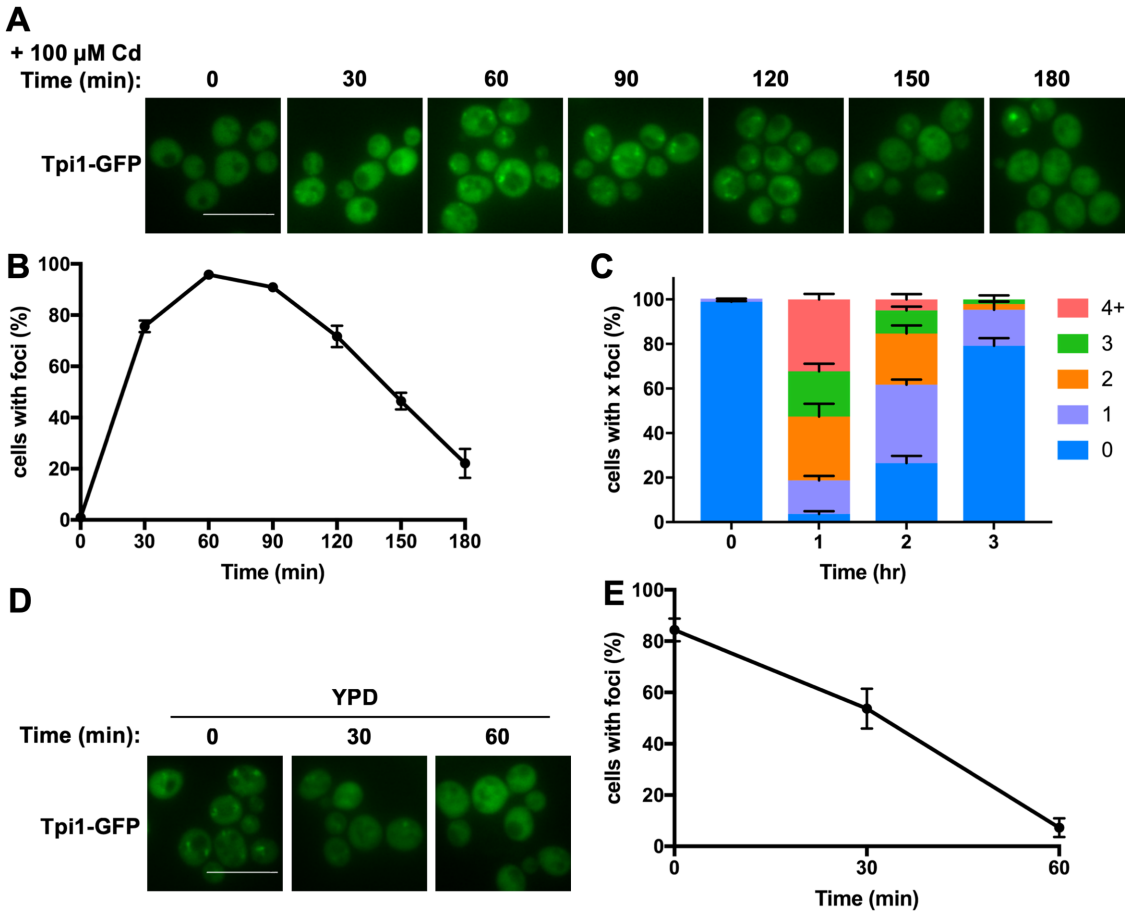

FIGURE 3: Cd-induced Tpi1-GFP aggregate formation and clearance dynamics. (A) Exponentially grown cells bearing Tpi1-GFP were incubated with 100 μM Cd and culture samples were visualized by live-cell fluorescence microscopy at 30-min intervals for 3 h. Representative images for the indicated time points are shown. Scale bar is 10 μm. (B) Quantitation of the mean percentage of total cells with foci from A at each time point ($n = 3$). (C) Quantitation of the relative percentage of cells from A with 1, 2, 3, or 4+ foci per cell following Cd exposure at the indicated timepoints ($n = 3$). (D) Exponentially grown cells bearing Tpi1-GFP were incubated in the presence of 100 μM Cd for 1 h to form aggregates, then transferred to medium lacking Cd for an additional 1 h. Representative images at the indicated 0, 30, and 60 min recovery timepoints are shown. Scale bar is 10 μm. (E) Quantitation of the mean percentage of total cells with foci following recovery ($n = 3$). A minimum of 100 cells were counted per biological replicate. Error bars indicate SD.

chaperones being recruited early to, if not seeding, sites of cadmium-induced protein aggregation.

Cadmium-induced folding sensitivity is thiol-dependent

A key feature of cadmium is its propensity to chelate exposed sulfhydryl groups. We therefore postulated that the aggregation dynamics we have established for Tpi1 was due to interactions with one or more of the cysteines previously found to be subject to oxidation (Le Moan *et al.*, 2006). The yeast Tpi1 enzyme is an active homodimer and contains two cysteine residues at positions 41 and 126 that are likely protected in the folded native conformation (Figure 5A; Lolis *et al.*, 1990). To determine whether the observed cadmium-induced aggregation is dependent on the presence of these cysteines, we made single and double alanine substitutions in the genomic GFP–protein fusion (C41A, C126A, and C41A C126A; Figure 5B). Expression and stability of all three cysteine mutants was comparable to that of the wild type and had no detectable effects on growth on glucose, a condition requiring a functional TPI enzyme (Figure 5, C and D; Compagno *et al.*, 2001). Under nonstress conditions, all three mutants were localized diffusely throughout the cytosol, similar to wild-type Tpi1-GFP, in agreement with our protein expression and cell viability data (Figure 5, E and F). Following 1 h of treatment with 100 μM $CdCl_2$, Tpi1-GFP bearing either single cysteine substitution aggregated at a level indistinguishable from that in the wild type. Strikingly, Tpi1-GFP C41A C126A failed to aggregate under the same conditions. These observations support our hypothesis that cadmium proteotoxicity is a thiol-dependent process and indicate that both cysteines must be present to confer folding sensitivity on Tpi1.

Thiol stress induced by glucose starvation

The Tpi1 cysteines appear to present a folding liability under challenge from thiol stress. Brandes *et al.* (2013) found that in chronologically aging yeast cultures the proteome undergoes thiol oxidation due to loss of reducing equivalents (NADPH) brought about by glucose depletion. Because at least one Tpi1 thiol (C126) had been identified previously as being oxidized in a thioredoxin mutant background (Le Moan *et al.*, 2006), we predicted that the redox imbalance in aging/starving cells may mimic thiol chelation by impacting Tpi1 cysteines. We monitored Tpi1-GFP aggregate

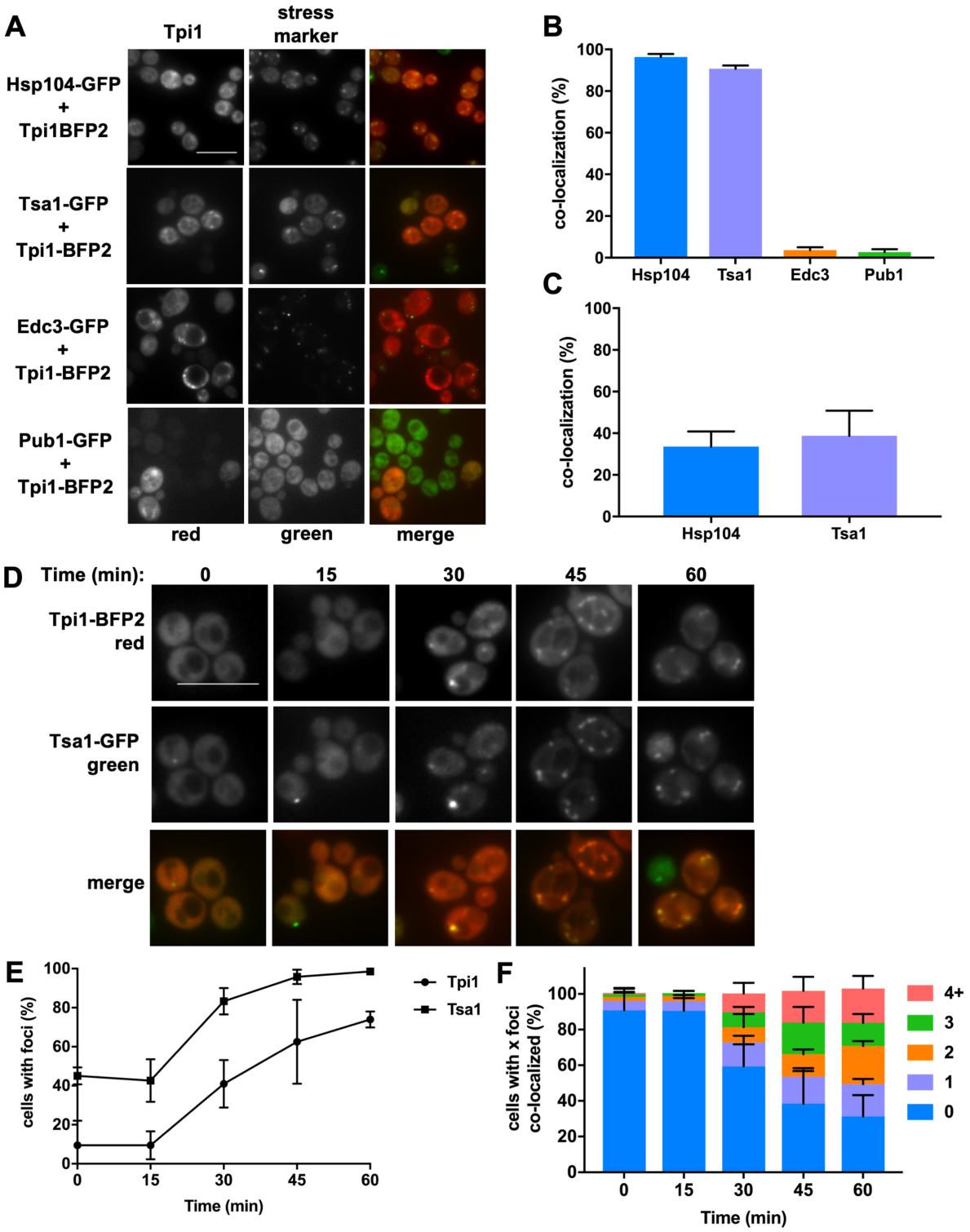

FIGURE 4: Tpi1-GFP recruits protein chaperones to foci distinct from other stress bodies. (A) Exponentially grown cells bearing GFP–protein fusions of Tsa1, Hsp104, Edc3, and Pub1 (stress marker, green) and also expressing Tpi1-BFP2 (Tpi1, false-colored red) on a plasmid were exposed to 750 µM Cd for 1 h and visualized by live-cell fluorescence microscopy. Representative images are shown. Scale bar: 10 µm. (B) Quantitation of the mean percent colocalization (merge) of Tpi1-BFP2 foci containing stress marker foci from A ($n = 3$). (C) Quantitation of the mean percentage colocalization of Tsa1- and Hsp104-GFP with Tpi1-BFP2 from A ($n = 3$). (D) Exponentially grown cells coexpressing Tsa1-GFP (green) and Tpi1-BFP2 (false-colored red) on a plasmid were exposed to 750 µM Cd for 1 h and visualized at 15-min intervals by live-cell fluorescence microscopy. (E) Quantitation of the mean percentage of total cells with foci from D at each time point ($n = 3$). (F) Quantitation of the relative percentage of cells from D with 1, 2, 3, or 4+ colocalized foci per cell following Cd exposure at the indicated timepoints ($n = 3$). A minimum of 100 cells were counted per biological replicate. Error bars indicate SD.

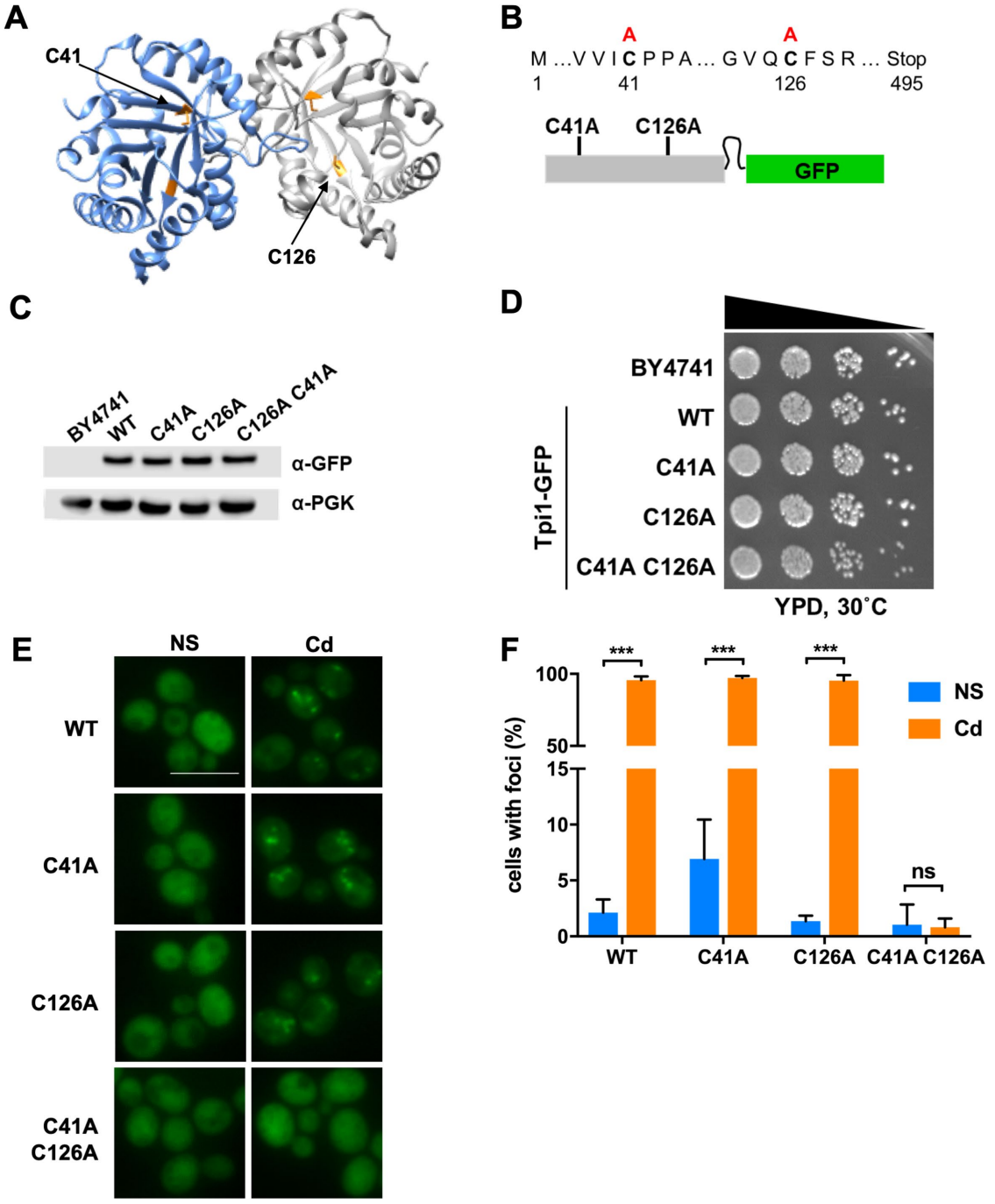

FIGURE 5: Cd-induced Tpi1-GFP aggregation requires cysteines 41 and 126. (A) Ribbon structure of the yeast Tpi1 homodimer with cysteines 41 and 126 indicated (orange) in each monomer (PDB: 1YPI). (B) Location of engineered alanine substitutions in chromosomal TPI1-GFP allele. (C) Western blot analysis of protein expression of Tpi1-GFP WT, C41A, C126A, and C41A C126A. α-GFP was used to identify the protein-GFP fusion and α-PGK was used as a load control. (D) Cell viability of Tpi1-GFP WT, C41A, C126A, and C41A C126A as determined by spot dilution assay. Wedge indicates serial 10-fold culture dilutions. (E) Exponentially grown cells bearing Tpi1-GFP WT, C41A, C126A, or C41A C126A were incubated in nonstress conditions (NS) or in the presence of 100 μM Cd for 1 h and visualized by live-cell fluorescence microscopy. Scale bar; 10 μm. (F) Quantitation of the mean percentage of total cells with foci ($n = 3$). Quantitation of the mean percentage of total cells with foci following recovery ($n = 3$). A minimum of 100 cells were counted per biological replicate. Error bars indicate SD. ns, not significant; ***, $p < 0.0001$.

formation in chronologically aging yeast under continuous culture in rich medium for 4 d (Figure 6, A–C). On day 1, as expected, we observed little to no aggregation of Tpi1-GFP, but as the days progressed, the percentage of cells with detectable aggregates steadily increased to a level comparable to that observed with cadmium treatment. Interestingly, glucose supplementation of the day 4 culture resulted in clearance of Tpi1-GFP aggregates, indicating that no additional aggregates were formed after glucose

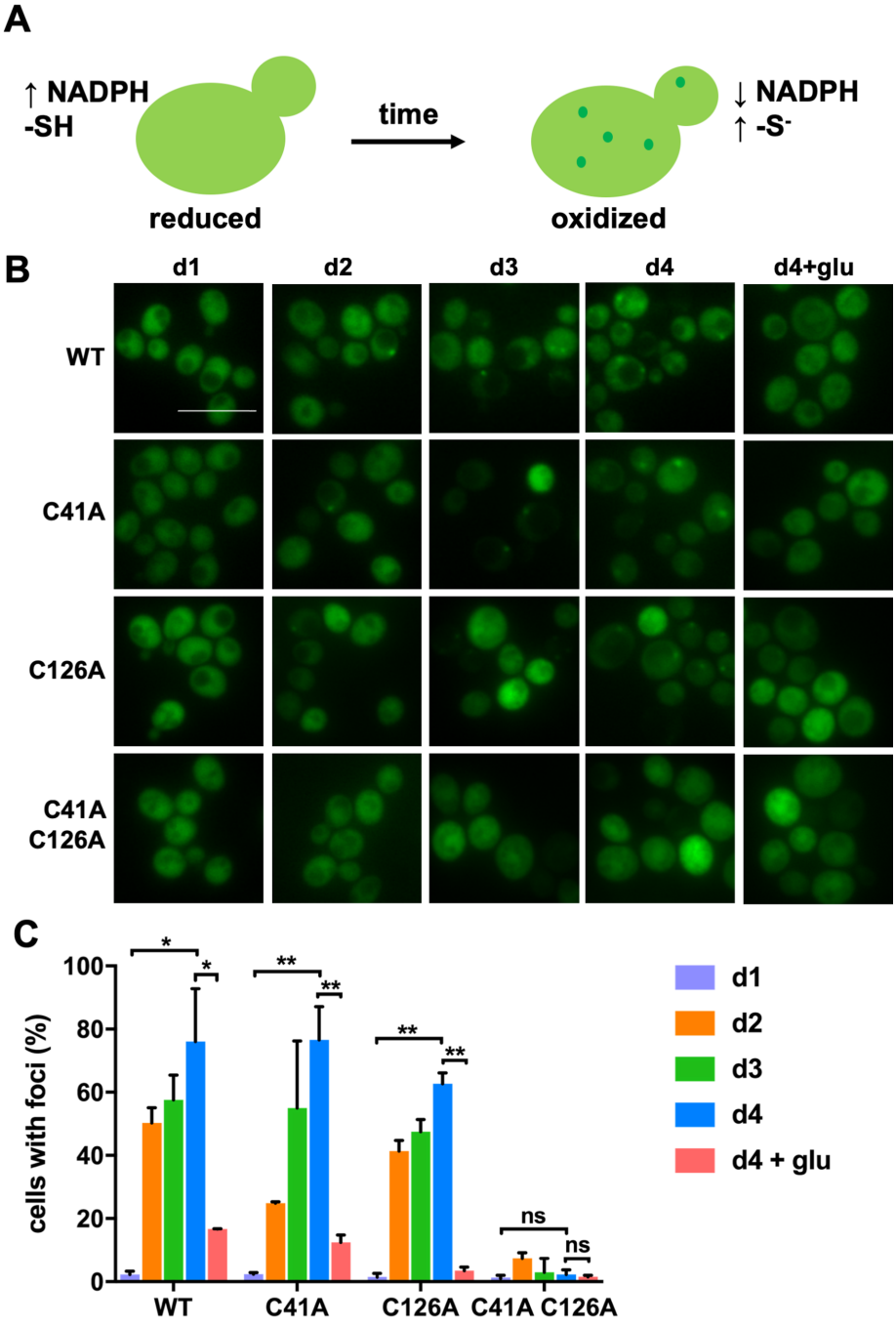

FIGURE 6: Chronological aging induces cysteine-dependent Tpi1-GFP aggregation. (A) Illustration of aging/starvation experiment. (B) Tpi1-GFP WT, C41A, C126A, and C41A C126A expressing cells were inoculated into rich medium and grown without additional supplementation for 4 d. On day 4, cells were supplemented with 2% glucose. Representative images from live-cell fluorescence microscopy are shown for each day (d1–d4) and after 1 h supplementation (d4+glu). Scale bar: 10 μm. (C) Quantitation of the mean percentage of total cells with foci for each strain ($n = 3$). A minimum of 100 cells were counted per biological replicate. Error bars indicate SD. ns, not significant; *, $p < 0.05$; **, $p < 0.001$.

addition and that previously existing aggregates were rapidly turned over.

To verify that the observed aggregation was indeed thiol-specific, we examined the cysteine mutants C41A, C126A, and C41A C126A. As observed with cadmium treatment, the behavior of Tpi1 with each single mutation was nearly identical to that of the wild type, while the double mutant displayed little to no focus formation over the course of the experiment. These findings are consistent with the model in which glucose starvation due to chronological aging induces thiol-specific stress, and in which at least in the case of Tpi1 two cysteines in the primary sequence of the protein render it folding-labile under such conditions.

Thiol-stress proteotoxicity is conserved between yeast and humans

Together with previous work, our findings suggest that cadmium is a potent proteotoxic agent in budding yeast, with particular affinity for nascent polypeptides. To extend these findings to humans, where cadmium is considered a deadly poison, we sought to monitor chaperone dynamics in human cells, utilizing HEK293 and HCT116 cell lines. We obtained a previously characterized carboxy-terminal YFP fusion to the human stress-inducible Hsp70 (HSPA1A) shown to localize to protein aggregates (Kim *et al.*, 2002). Plasmids expressing Hsp70-YFP or YFP alone were transfected into cells and expression was assessed by Western blot and fluorescence microscopy. Western blot analysis validated a similar expression level in both cell lines (Figure 7A). Cadmium treatment clearly induced the heat shock response in both lines, as demonstrated by quantitative reverse transcription-PCR (qRT-PCR) of the stress-induced genes DNAJ1B (Hsp40) and HSPA1A (Hsp70) following exposure to either heat shock or $CdCl_2$ (Supplemental Figure S3). Under nonstress conditions, Hsp70-YFP was localized diffusely throughout the cytosol and mostly excluded from the nucleus (Figure 7, B and E). We noted a consistent low level of both YFP and Hsp70-YFP foci (~1–5) in the absence of stress, likely attributable to transient overexpression, and therefore chose to quantify aggregation only in cells exhibiting >5 foci. Following exposure to 50 μM $CdCl_2$ for 6 h, distribution of YFP alone remained unchanged, while Hsp70-YFP formed multiple foci per cell in both cell lines, consistent with Hsp70 localizing to thiol stress–induced protein aggregates. These findings establish that cadmium is a proteotoxic agent in human cells as it is in yeast.

Next, we were interested in determining whether the Tpi1 folding sensitivity we observed in budding yeast was conserved between yeast and humans. We constructed an amino-terminal GFP fusion to the human homologue (hTPI) produced from a mammalian constitutive expression vector. GFP-hTPI and GFP alone were transfected into HEK293 and HCT116 cell lines and expression was confirmed by Western blot and fluorescence microscopy (Figure 7C). While GFP alone remained diffuse under both nonstress and

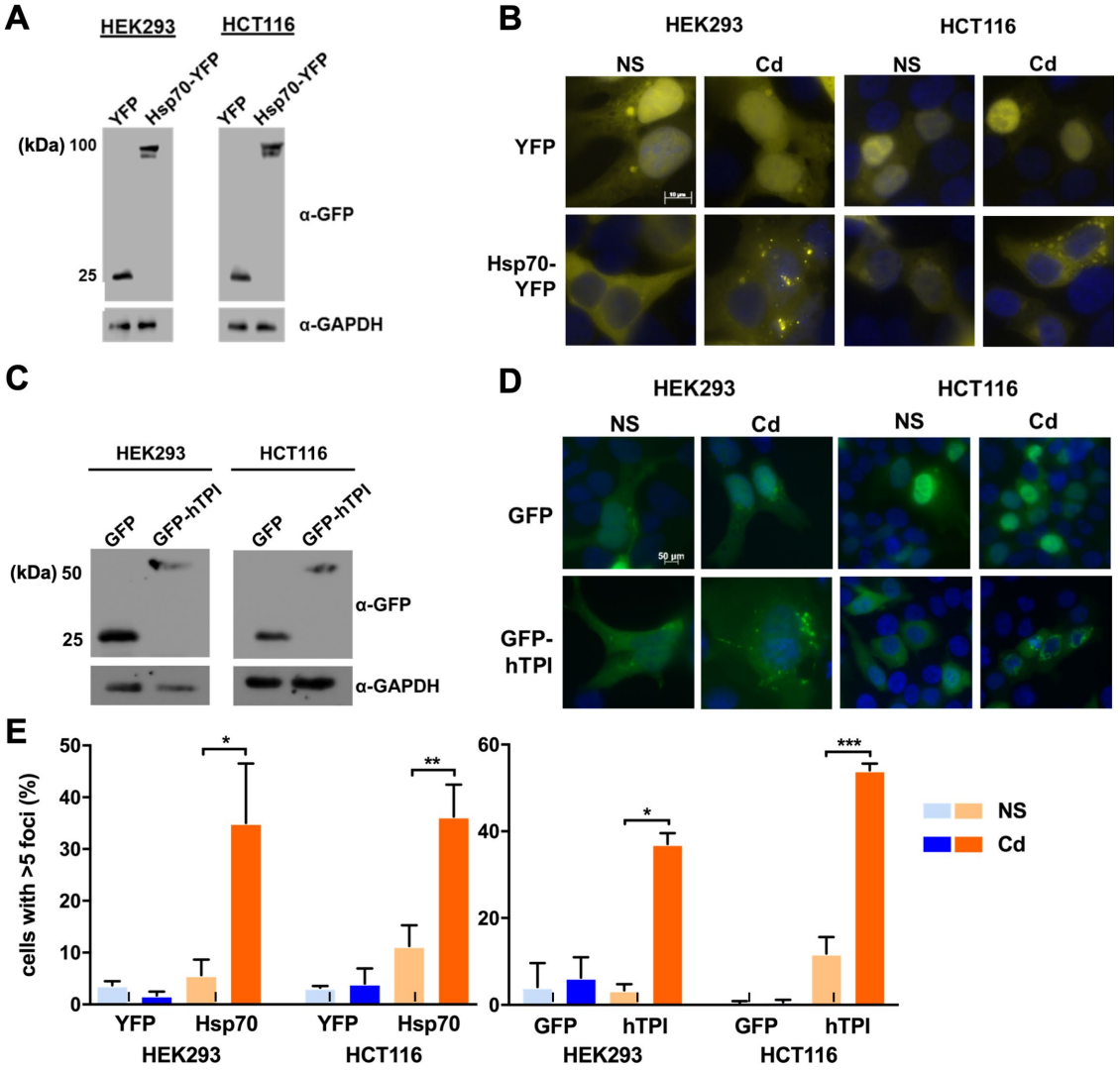

FIGURE 7: Cd proteotoxicity is conserved between yeast and human cells. (A) Western blot analysis of HEK293 and HCT116 cells expressing either Hsp70-YFP or YFP alone. α-GFP was used to detect Hsp70-YFP and YFP and α-GAPDH was used as a loading control. (B) HEK293 and HCT116 cells expressing Hsp70-YFP or YFP alone were incubated at 37°C with (Cd) or without (NS) 50 μM Cd for 6 h. Following incubation, cells were fixed, stained with DAPI, and visualized by fluorescence microscopy. Representative images of each cell type for each condition are shown as indicated. Scale bar: 50 μm. (C) Western blot analysis of HEK293 and HCT116 cells expressing GFP-hTPI or GFP alone. α-GFP was used to detect GFP-hTPI and GFP and α-GAPDH was used as a loading control. (D) HEK293 and HCT116 cells expressing GFP-hTPI and GFP alone were incubated at 37°C with (Cd) or without (NS) 50 μM Cd for 6 h. Following incubation, cells were fixed, stained with DAPI, and visualized by fluorescence microscopy. Representative images of each cell type for each condition are shown as indicated. Scale bar: 50 μm. (E) Quantitation of the mean percentage of cells with >5 foci per cell ($n = 3$). A minimum of 100 cells were counted per biological replicate. Error bars indicate SD. ns, not significant; *, $p < 0.05$, **; $p < 0.001$; ***, $p < 0.0001$.

cadmium-stress conditions, GFP-hTPI formed a large number of aggregates per cell, indicating that human TPI, like the yeast homologue, is highly susceptible to cadmium-induced aggregation (Figure 7, D and F).

DISCUSSION

Our study extends preceding findings that thiol-specific stresses brought about by the heavy metal cadmium or glucose starvation are proteotoxic. Previous work had relied exclusively on the use of protein quality control factors such as Hsp104 to serve as a proxy for the impacts of these environmental insults on the proteome. While informative and important, the identity of endogenous proteins and the extent to which they are affected by thiol stress remained unexplored. Identification of Tpi1 in budding yeast as one such protein allowed confirmation of several previous observations. First, previous work had demonstrated that only nascent polypeptide emerging from the ribosome may be susceptible to thiol stress, as Hsp104-GFP localization to aggregates is inhibited by pretreatment with cycloheximide to block translation (Jacobson *et al.*, 2017). Our finding that Tpi1 exhibits the same behavior suggests that exposure to thiol-chelating elements such as cadmium may result at least in transient modification or interaction with temporarily exposed cysteine thiols. These nonnative circumstances would therefore result in an inability to fold properly, leading to the formation of protein

aggregates and the recruitment of chaperones such as Hsp104 and Tsa1. These chaperones in particular are considered markers of protein quality control, or "Q"-bodies that consolidate misfolded proteins for delivery to protein degradation compartments such as the JUNQ/INQ structure (Escusa-Toret *et al.*, 2013). We demonstrated that Tpi1-GFP colocalizes with Hsp104 and Tsa1, and not markers for stress granules or P-bodies. Taking these results together with previous observations that protein degradation mutants (*ubc7*, *pre1-1*, *rpn4Δ*) exhibit cadmium hypersensitivity and aggregation persistence (Jungmann *et al.*, 1993; Jacobson *et al.*, 2012, 2017), we propose that foci observed in the presence of cadmium represent terminally misfolded proteins destined for degradation rather than adaptive transient assemblies.

We were initially puzzled to find that of the 10 candidates evaluated in our pilot screen with demonstrated redox-active cysteines, we identified only the glycolytic enzyme Tpi1 as folding-sensitive in response to cadmium exposure. Our fluorescence microscopy approach was chosen to allow detection of even minor aggregation, on the assumption that a positive signal of focus formation against a diffuse background would be clearly visible. In support of our hypothesis, this approach allowed us to visualize aggregation of the population of Tpi1 synthesized in the presence of cadmium over a 30-min period. While our proof-of-principle analysis was by no means exhaustive, we conclude that misfolding in response to thiol stress in the cytoplasm may in fact be a relatively uncommon property, even among redox-active proteins. This is in contrast to the parallel scenario in the endoplasmic reticulum, where the majority of resident and secreted proteins contain one or more disulfide bonds that when disrupted genetically or pharmacologically result in severe misfolding and overall proteotoxicity (Walter and Ron, 2011). However, given the clear recruitment of chaperones to cytoplasmic aggregates in both yeast and human cells, there are likely to be additional individual proteins whose folding is negatively impacted by thiol oxidization or modification. An obvious next step in identifying such targets is the use of high-sensitivity quantitative mass spectrometry, which may have a resolution capable of detecting partitioning of misfolded nascent chains into the insoluble fraction.

A critical advantage of identifying a specific target of cadmium proteotoxicity was the opportunity to test the proposed mechanism of cysteine thiol chelation via mutagenesis. Previous work had established that arsenic, another toxic heavy metal with significant thiol reactivity, inhibited protein folding activity of the bacterial Hsp70 system in vitro (Jacobson *et al.*, 2012). Therefore, recruitment of Hsp104-GFP into cytoplasmic foci could have several possible mechanistic explanations. We observed that simultaneous replacement of both C41 and C126with alanine in Tpi1-GFP, but not of either cysteine alone, abrogated aggregate formation in response to both cadmium and glucose starvation.

The presence of a single cysteine therefore renders Tpi1 susceptible to misfolding and aggregation. Cadmium inhibition of the proteasome or chaperones would not have produced this outcome ,as this would lead to Tpi1 folding sensitivity regardless of the presence or absence of the cysteines, strongly supporting a model where cadmium interacts directly with at least one cysteine per Tpi1 polypeptide chain to disrupt folding. Scenarios where cadmium may form multidentate complexes with multiple peptide chains cannot be ruled out. It is also important to note that these potential mechanisms are not mutually exclusive—cadmium-induced aggregates may form via metal–thiol complexes and be transiently stabilized via inhibition of other components of the protein quality control system. While clearly also cysteine-dependent, the mechanism behind Tpi1-GFP aggregation in aging cell cultures is likely to be more indirect. Depletion of glucose over time results in a loss of reducing equivalents (e.g., NADPH) that are used to power thiol reduction by the thioredoxin system (Morano *et al.*, 2012; Brandes *et al.*, 2013). Inability to maintain a reducing environment in the cytosol leads to oxidation of protein thiols, which in the case of Tpi1-GFP promotes misfolding and aggregation.

An important component of the present study is the determination that cadmium stress is proteotoxic in human cells as well as in yeast. While cadmium and ROS have long been known to be potent inducers of heat shock response in human and other animal cell types, to our knowledge ours is the first demonstration of cadmium-induced protein aggregate formation in human cells, as evidenced using Hsp70 as a proxy for localization of misfolded proteins. Moreover, the TPI enzyme, itself highly homologous between yeast and humans (53% identity, 68% similarity), appears also to be aggregation-prone in response to cadmium in human cell lines. Although the structure and enzymatic function of Tpi1 are conserved, the number of cysteine residues is not. In addition to the two conserved positions (C41 and C126), human TPI possesses an additional three cysteines (C66, C86, and C280) that may react with cadmium. In this study, we did not explore the requirement for one or multiples of the five cysteine residues to confer misfolding sensitivity to cadmium; however, we speculate that a similar thiol-dependent mechanism may be in play. It is worth noting that the mutation C41Y has been found in patients with the rare disease triose phosphate isomerase deficiency (Ralser *et al.*, 2006). Reduced function of this key glycolytic enzyme leads to progressive neurodegeneration, or in the case of compound heterozygous mutations, early childhood lethality (Arya *et al.*, 1995). Intriguingly, evidence suggests that some hypomorphic alleles of TPI may impede dimerization of the enzyme, leading to misfolding and aggregate formation, rather than solely reducing catalytic activity (Oláh *et al.*, 2002; Ralser *et al.*, 2006). Together with our data, these results suggest that despite its high cellular abundance and clear metabolic importance, TPI may be a folding-labile protein sensitive to environmental imbalance as well as genetic perturbation, highlighting its uniqueness compared with other proteins screened in this study (e.g., Sod1). Our findings also emphasize the value of investigating fundamental aspects of proteostasis in a model system as an avenue to understanding the molecular mechanisms behind toxicity of environmental pollutants such as heavy metals and organic electrophilic agents.

MATERIALS AND METHODS

Strains and plasmids

Yeast. All yeast-genomic GFP–protein fusion strains used in this study were obtained from the genomic GFP–protein fusion library (Invitrogen; Howson *et al.*, 2005). To construct cysteine substitution mutants of Tpi1 (C41A, C126A, and C41A C126A), the p*TPI1-TPI*-GFP::*HISMX6* sequence was amplified using PCR from genomic DNA of the Tpi1-GFP strain and cloned using homologous recombination into the yeast expression vector p416. Cysteine-to-alanine replacement mutations were introduced into the p416*TPI-tpi1*-GFP vector using the QuickChange Lightning Site-directed Mutagenesis kit and protocol (Agilent). Mutants were verified by DNA sequencing. Each mutant *tpi1*-GFP::*HISMX6* allele was amplified from plasmids by PCR and inserted into the BY4741 (*MATa his3Δ0 leu2Δ0 met15Δ0 ura3Δ0*) parent strain chromosome using homologous recombination at the *TPI1* locus. Integration of mutants was confirmed by DNA sequencing. Yeast expression vectors used in this study were the following: p416*TEF*-GFP, p416*TEF*-mTagBFP2, and p416*TEF-tpi1*-mTagBFP2. The GFP and mTagBFP2 fluorescent protein tags were amplified from the pFA6a-link-yomTagBFP2

(Addgene; Lee *et al.*, 2013) and p416*CUP1*-GFP (Abrams *et al.*, 2014) plasmids by PCR and cloned into the p416*TEF* vector. All plasmids were constructed using standard restriction enzyme–based cloning methods. The following mammalian expression vectors were used in this study: p*CMV*-EGFP-C1 and p*CMV*-EYFP-N1 (Clontech), p*CMV*-Hsp70-EYFP (Kim *et al.*, 2002), and p*CMV*-EGFP-hTPI. The p*CMV*-EGFP-hTPI plasmid was constructed by amplifying the human TPI coding sequence (*hTPI*) from cDNA (HeLa) and cloning into the p*CMV*-EGFP-C1 vector. All plasmid constructs were verified by enzyme digestion and DNA sequencing.

Human cells. The human cell lines HEK293 (transformed human embryonic kidney cells; American Type Culture Collection [ATCC]) and HCT116 (human colorectal carcinoma cells; ATCC) were used in this study. Cells were seeded at 150,000–250,000 cells/well in six-well tissue culture–treated plates and incubated at 37°C with 5% CO_2 in DMEM high glucose (Hyclone) supplemented with 5% fetal bovine serum (FBS; Hyclone) and penicillin–streptomycin. At 50% confluence, cells were transfected with the desired expression vector using JetPrime transfection reagent according to the manufacturer's optimized protocol for each cell line (Polyplus Transfection).

Cell growth conditions and treatments

Yeast. All strains used were grown in YPD (1% yeast extract, 2% peptone, 2% glucose) liquid growth medium at 30°C with aeration to logarithmic phase (OD_{600} 0.4–0.8). For thiol-stress treatment, strains were incubated with $CdCl_2$ (25–1000 μM) for 0–3 h. For the cycloheximide chase experiment, strains were incubated with 0.1 mg/ml cycloheximide for 15 min before addition of 100 μM $CdCl_2$ for 1 h. For glucose starvation/chronological aging, cells were incubated in a 30°C shaking incubator for 4 d and supplemented with 2% dextrose on day 4 for 1 h. For yeast spot assays, serial dilutions of each strain were made (10^{-1}–10^{-5}) and plated on YPD medium using a 96-well plate and a metal pronged grid. Plates were incubated at 30°C and then imaged after 3 d.

Human cells. The HEK293 and HCT116 cell lines were seeded at 150,000–250,000 cells/well in six-well tissue culture–treated plates and incubated in standard growth medium (DMEM high glucose, 5% FBS, and penicillin–streptomycin) at 37°C 5% CO_2. For heat shock treatment, 60–80% confluent plates were incubated on a metal-plated shelf at 43°C 5% CO_2 for 1 h. For cadmium treatment, 60–80% confluent plates were incubated at 37°C, 5% CO_2 with 50 μM $CdCl_2$ for 6 h.

Protein expression

Yeast. Cell lysates were obtained by lysing 6 OD units of cells using the glass-bead cell lysis procedure (Abrams *et al.*, 2014). The protein concentration was determined by the Bradford assay (Bio-Rad) in a microplate reader (Synergy MX, Biotek). Protein samples were boiled in SDS–PAGE sample-loading buffer and stored at –20°C. Equal protein concentrations of each sample were loaded onto 12% bis-acrylamide/SDS gel and separated by gel electrophoresis. Separated protein samples were transferred to a polyvinylidene difluoride (PVDF) membrane and blotted with monoclonal α-GFP (Roche) to detect the GFP fusion protein. Monoclonal α-PGK (Invitrogen) was used as a loading control.

Human cell lines. HEK293 and HCT116 cell lines expressing the desired vectors were detached from dishes using trypsin, washed with phosphate-buffered saline (PBS), and lysed in RIPA buffer (10 mM Tris–HCl [pH 8.0], 1 mM EDTA, 1% Triton X-100, 0.1% sodium deoxycholate, 0.1% SDS, 140 mM NaCl, and PIC) for 15 min on ice. Lysates were cleared by centrifugation at 15,000 rpm at 4°C for 10 min. The concentration of protein was calculated with the BCA assay (Bio-Rad). Equal concentrations of each sample were loaded onto 12% bis-acrylamide/SDS gel and separated by gel electrophoresis. Separated protein samples were transferred to a PVDF membrane and blotted with monoclonal α-GFP (Roche) to detect the FP fusion protein. α-GAPDH (Santa Cruz Biotechnology) was used as a loading control.

Fluorescence microscopy

Yeast live cell imaging. For all experiments, live cells were wet-mounted on glass slides and imaged immediately using an Olympus IX81 microscope with a 100× objective with FITC filters to detect GFP and a standard UV/4′,6-diamidino-2-phenylindole (DAPI) filter to detect BFP2. Within each experiment, cells were imaged with identical exposure times.

Fixed human cell imaging. HEK293 and HCT116 cell lines were seeded onto glass coverslips in tissue culture–treated six-well plates. The following day, cells were transfected with desired expression vectors. On day 3, cells were exposed to the conditions described above, fixed onto coverslips using 4% paraformaldehyde in PBS, incubated with Hoescht/DAPI stain for nuclear DNA detection, and mounted on glass slides using VectaShield mounting medium. For each cell type and experimental growth condition, slides were imaged at 63× magnification in multiple Z-planes using a Zeiss Axioskop40 microscope. Appropriate filter sets were used as above.

Cryolysis and differential centrifugation

This method of cell lysis and fractionation was adapted from Wallace *et al.* (2015). Approximately 18 OD units of cells were incubated in YPD medium, with or without 750 μM $CdCl_2$, for 1 h at 30°C. Treated cells were collected, washed, resuspended in 100 μl of lysis buffer (20 mM Tris-HCl [pH 7.9], 0.5 mM EDTA, 10% glycerol, 50 mM NaCl, and protease inhibitor cocktail [PIC; Abrams *et al.*, 2014]), and flash frozen in liquid nitrogen. Glass beads were added to frozen cell pellets and switched from vortex to dry ice for 1-min intervals six times. Following lysis, 200 μl of lysis buffer was added to each sample, the samples were then thawed on ice, and cellular debris was separated from the cell lysate by slow spinning at 3000 × *g* at 4°C for 30 s.

Extracted total protein lysate was separated into soluble and insoluble fractions by ultracentrifugation at 100,000 × *g* at 4°C for 20 min. The supernatant (soluble) fraction was transferred to a new microcentrifuge tube. The insoluble fraction pellets were washed with lysis buffer, centrifuged again at 100,000 × *g* 4°C for 20 min, and decanted. Washed pellets were sonicated in 50 μl of insoluble protein buffer (8 M urea, 20 mM Tris-HCl [pH 7.4], 150 mM NaCl, 2 mM EDTA, 2% SDS, and PIC) for 10 min in an ambient-temperature water bath sonicator and centrifuged at 20,000 × *g* at ambient temperature for 5 min. Both soluble and insoluble fractions were boiled in SDS–PAGE sample loading buffer and stored at –20°C.

qRT-PCR

HEK293 and HCT116 cells were seeded at 150,000–250,000 cells/well in six-well tissue culture–treated plates containing standard growth medium. At 50–70% confluence, cells were incubated in the growth conditions described above. All treatments were recovered for 6 h at 37°C 5% CO_2. Following treatment, cells were detached from the dish using trypsin, washed with PBS, and frozen on dry ice. Frozen cell pellets were stored at –80°C until processing.

RNA was extracted from treated cell pellets using the TRIZOL reagent (Thermo Fisher). The RNA concentration was calculated

using absorbance at 260 nm (peak), 280 nm (ratio), and 320 nm (ref.) determined using a nanodrop plate reader (Synergy MX; Biotek), and 10–20 µg of each sample was treated with Turbo DNase (Invitrogen). Following DNase treatment, RNA was purified by phenol/chloroform extraction, the concentration was calculated as before, and 1 µg of RNA was converted to cDNA using the iScript cDNA synthesis kit and protocol (Bio-Rad). mRNA expression of the Hsf1-induced genes *HSPA1A* (HSP70) and *DNAJ1A* (HSP40) was measured by quantitative, real-time PCR using iTaq Universal SYBR Green Supermix (Bio-Rad) and calculated using standard methods (Nolan *et al*., 2006). mRNA expression of *GAPDH* was used as a normalization control.

Statistical analysis

Statistical significance was determined using an unpaired Student's *t* test with Welch's correction performed using QuickCalcs and Prism (version 7.0c, GraphPad Software).

ACKNOWLEDGMENTS

A.E.F. and K.A.M. were supported by National Institutes of Health (NIH) GM127287. C.D. was supported by funds from UT McGovern Medical School. We are indebted to Paul Herman of The Ohio State University for sharing GFP reagents. The molecular graphics image was produced using the UCSF Chimera package from the Computer Graphics Laboratory, University of California, San Francisco (supported by NIH P41 RR-01081).

REFERENCES

Abrams JL, Verghese J, Gibney PA, Morano KA (2014). Hierarchical functional specificity of cytosolic heat shock protein 70 (Hsp70) nucleotide exchange factors in yeast. J Biol Chem 289, 13155–13167.

Arya R, Layton DM, Bellingham AJ (1995). Hereditary red cell enzymopathies. Blood Rev 9, 165–175.

Brandes N, Reichmann D, Tienson H, Leichert LI, Jakob U (2011). Using quantitative redox proteomics to dissect the yeast redoxome. J Biol Chem 286, 41893–41903.

Brandes N, Tienson H, Lindemann A, Vitvitsky V, Reichmann D, Banerjee R, Jakob U (2013). Time line of redox events in aging postmitotic cells. Elife 2, e00306.

Buchan JR, Muhlrad D, Parker R (2008). P bodies promote stress granule assembly in *Saccharomyces cerevisiae*. J Cell Biol 183, 441–455.

Chen B, Retzlaff M, Roos T, Frydman J (2011). Cellular strategies of protein quality control. Cold Spring Harb Perspect Biol 3, a004374.

Compagno C, Brambilla L, Capitanio D, Boschi F, Maria Ranzi B, Porro D (2001). Alterations of the glucose metabolism in a triose phosphate isomerase-negative *Saccharomyces cerevisiae* mutant. Yeast 18, 663–670.

Escusa-Toret S, Vonk WIM, Frydman J (2013). Spatial sequestration of misfolded proteins by a dynamic chaperone pathway enhances cellular fitness during stress. Nat Cell Biol 15, 1231–1243.

Ghaemmaghami S, Huh W-K, Bower K, Howson RW, Belle A, Dephoure N, O'Shea EK, Weissman JS (2003). Global analysis of protein expression in yeast. Nature 425, 737–741.

Hanzén S, Vielfort K, Yang J, Roger F, Andersson V, Zamarbide-Fores S, Andersson R, Malm L, Palais G, Biteau B, *et al*. (2016). Lifespan control by redox-dependent recruitment of chaperones to misfolded proteins. Cell 166, 140–151.

Howson R, Huh W-K, Ghaemmaghami S, Falvo JV, Bower K, Belle A, Dephoure N, Wykoff DD, Weissman JS, O'Shea EK (2005). Construction, verification and experimental use of two epitope-tagged collections of budding yeast strains. Comp Funct Genomics 6, 2–16.

Jacobson T, Navarrete C, Sharma SK, Sideri TC, Ibstedt S, Priya S, Grant CM, Christen P, Goloubinoff P, Tamás MJ (2012). Arsenite interferes with protein folding and triggers formation of protein aggregates in yeast. J Cell Sci 125, 5073–5083.

Jacobson T, Priya S, Sharma SK, Andersson S, Jakobsson S, Tanghe R, Ashouri A, Rauch S, Goloubinoff P, Christen P, Tamás MJ (2017). Cadmium causes misfolding and aggregation of cytosolic proteins in yeast. Mol Cell Biol 37, e00490-16.

Jang HH, Lee HO, Chi YH, Jung BG, Park SK, Park JH, Lee JR, Lee SS, Moon JC, Yun JW, *et al*. (2004). Two enzymes in one: two yeast peroxiredoxins display oxidative stress-dependent switching from a peroxidase to a molecular chaperone function. Cell 117, 625–635.

Jungmann J, Reins H-A, Schobert C, Jentsch S (1993). Resistance to cadmium mediated by ubiquitin-dependent proteolysis. Nature 361, 369–371.

Kim S, Nollen EAA, Kitagawa K, Bindokas VP, Morimoto RI (2002). Polyglutamine protein aggregates are dynamic. Nat Cell Biol 4, 826–831.

Kshirsagar M, Parker R (2004). Identification of Edc3p as an enhancer of mRNA decapping in *Saccharomyces cerevisiae*. Genetics 166, 729–739.

Lee S, Lim WA, Thorn KS (2013). Improved blue, green, and red fluorescent protein tagging vectors for *S. cerevisiae*. PLoS One 8, e67902.

Le Moan N, Clement G, Le Maout S, Tacnet F, Toledano MB (2006). The *Saccharomyces cerevisiae* proteome of oxidized protein thiols: contrasted functions for the thioredoxin and glutathione pathways. J Biol Chem 281, 10420–10430.

Lolis E, Alber T, Davenport RC, Rose D, Hartman FC, Petsko GA (1990). Structure of yeast triosephosphate isomerase at 1.9-Å resolution. Biochemistry 29, 6609–6618.

Miller SBM, Ho CT, Winkler J, Khokhrina M, Neuner A, Mohamed MY, Guilbride DL, Richter K, Lisby M, Schiebel E, *et al*. (2015). Compartment-specific aggregases direct distinct nuclear and cytoplasmic aggregate deposition. EMBO J 34, 778–797.

Morano KA, Grant CM, Moye-Rowley WS (2012). The response to heat shock and oxidative stress in *Saccharomyces cerevisiae*. Genetics 190, 1157–1195.

Nolan T, Hands RE, Bustin SA (2006). Quantification of mRNA using real-time RT-PCR. Nat Protoc 1, 1559–1582.

Oláh J, Orosz F, Keserü GM, Kovári Z, Kovács J, Hollán S, Ovádi J (2002). Triosephosphate isomerase deficiency: a neurodegenerative misfolding disease. Biochem Soc Trans 30, 30–38.

Ralser M, Heeren G, Breitenbach M, Lehrach H, Krobitsch S (2006). Triose phosphate isomerase deficiency is caused by altered dimerization—not catalytic inactivity—of the mutant enzymes. PLoS One 1, e30.

Saad S, Cereghetti G, Feng Y, Picotti P, Peter M, Dechant R (2017). Reversible protein aggregation is a protective mechanism to ensure cell cycle restart after stress. Nat Cell Biol 19, 1202–1213.

Sharma SK, Goloubinoff P, Christen P (2008). Heavy metal ions are potent inhibitors of protein folding. Biochem Biophys Res Commun 372, 341–345.

Tamás MJ, Sharma SK, Ibstedt S, Jacobson T, Christen P (2014). Heavy metals and metalloids as a cause for protein misfolding and aggregation. Biomolecules 4, 252–267.

Toledano MB, Delaunay-Moisan A, Outten CE, Igbaria A (2013). Functions and cellular compartmentation of the thioredoxin and glutathione pathways in yeast. Antioxid Redox Signal 18, 1699–1711.

Trott A, West JD, Klaićl, Westerheide SD, Silverman RB, Morimoto RI, Morano KA (2008). Activation of heat shock and antioxidant responses by the natural product celastrol: transcriptional signatures of a thiol-targeted molecule. Mol Biol Cell 19, 1104–1112.

Wallace EWJ, Kear-Scott JL, Pilipenko EV, Schwartz MH, Laskowski PR, Rojek AE, Katanski CD, Riback JA, Dion MF, Franks AM, *et al*. (2015). Reversible, specific, active aggregates of endogenous proteins assemble upon heat stress. Cell 162, 1286–1298.

Walter P, Ron D (2011). The unfolded protein response: from stress pathway to homeostatic regulation. Science 334, 1081–1086.

Wang Y, Gibney PA, West JD, Morano KA (2012). The yeast Hsp70 Ssa1 is a sensor for activation of the heat shock response by thiol-reactive compounds. Mol Biol Cell 23, 3290–3298.

Weids AJ, Grant CM (2014). The yeast peroxiredoxin Tsa1 protects against protein-aggregate-induced oxidative stress. J Cell Sci 127, 1327–1335.

Weids AJ, Ibstedt S, Tamás MJ, Grant CM (2016). Distinct stress conditions result in aggregation of proteins with similar properties. Sci Rep 6, 1–12.

West JD, Wang Y, Morano KA (2012). Small molecule activators of the heat shock response: chemical properties, molecular targets, and therapeutic promise. Chem Res Toxicol 25, 2036–2053.